

Electron tunneling into superconducting CeRu₂

Toshikazu Ekino and Hironobu Fujii

Faculty of Integrated Arts and Sciences, Hiroshima University, Higashi-Hiroshima 739, Japan

Takao Nakama and Katsuma Yagasaki

College of Science, University of Ryukyus, Okinawa 903-01, Japan

(Received 16 December 1996; revised manuscript received 15 May 1997)

The superconducting energy gap of CeRu₂ has been studied by break-junction tunneling. The observed gap values $2\Delta(0)=1.9\text{--}2.6$ meV with $T_c=5.4\text{--}6.7$ K give the ratio $2\Delta(0)/k_B T_c=4.1\text{--}4.4$, indicating a strong-coupling superconductor. The temperature dependence of the gap value is in good agreement with the BCS prediction. [S0163-1829(97)02037-7]

Recently, much attention has been paid to superconductivity in the cubic-Laves-phase compound CeRu₂ for its possible exisotic superconducting phase occurring near the upper critical field.¹ This compound exhibits the superconducting transition temperature T_c of 6 K, which is the highest value among the Ce intermetallic superconductors. Specific-heat measurements have revealed a linear electronic coefficient γ of $29\text{ mJ K}^{-2}\text{ mol}^{-1}$ and the discontinuity at $T_c\Delta C=2\gamma T_c$.² The NMR measurements have shown a Hebel-Slichter peak and the ratio $2\Delta(0)/k_B T_c=4$, where $2\Delta(0)$ is the superconducting energy gap at 0 K.³ These results are consistent with the picture of a strong-coupling superconductor for CeRu₂.

In this paper we report tunneling measurements of CeRu₂ to clarify the nature of its superconductivity in a more direct way. Tunneling is the most successful technique used to measure the quasiparticle energy gap. The present work allows us to make a quantitative analysis based on BCS theory. The results presented here, giving essential knowledge of its superconductivity, will be also helpful to investigate what occurs in mixed states.

Fabrication of the artificial tunneling barrier on the Ce-based compounds has been difficult because of their reactive surface characteristics. One of the solutions is to use the *in situ* break junction. Since this technique provides the cleanest junction, the essential features can be obtained. For the measurements, polycrystalline samples having a *bulk* $T_c=6$ K with a resistive transition width of <0.2 K were used, which were prepared by arc melting of a stoichiometric ratio of Ce(4*N*) and Ru(3*N*), and annealing for 1 week at 1000°C .¹ The junctions were formed by cracking the sample on the glass-fiber substrate below the liquid-helium temperature. The tunneling conductance $dI(V)/dV$ as a function of bias voltage (V) was measured by an ac modulation technique using a four-probe method.

In this work, substantial gap distributions at a low temperature were observed for samples which had been confirmed to be single phase by x-ray diffraction. These are found to be due to local T_c distributions that could not be detected by a superconducting quantum interference device (SQUID), because of the microscopic nature of inhomogeneities which could not be readily observable in the bulk sample. Such T_c distributions have also been found in the

other intermetallic superconductors,⁴ and they are due to the particular property of the break junction that is sensitive to the local change in stoichiometry at the surface regions. The highest T_c value in the present tunneling measurements is 6.7 K, which is well above the bulk T_c value. A similar value has been in fact observed by the susceptibility.⁵ Further, such a value has been obtained in $\text{Ce}_{1-x}\text{La}_x\text{Ru}_2$ for small x , suggesting that rather small local variations in the electronic properties easily induce a substantial T_c change.⁶

Figure 1 shows the tunneling conductances $dI(V)/dV$ from different break junctions. The conductance fitting results are presented by the dashed lines. For the fitting of the superconductor-insulator-superconductor (SIS) tunneling [Figs. 1(a) and 1(b)], the conductance is calculated using the expression⁷

$$dI(V)/dV = C \int_{-\infty}^{+\infty} \{N(E, \Gamma) [dN(E+eV, \Gamma)/dV] \\ \times [f(E) - f(E+eV)] + N(E, \Gamma) N(E+eV, \Gamma) \\ \times [-df(E+eV)/dV]\} dE, \quad (1)$$

where C , $N(E, \Gamma)$, and $f(E)$ are the scaling parameter, the broadened BCS density of states proposed by Dynes *et al.*⁸

$$N(E, \Gamma) = |\text{Re}\{(E - i\Gamma)/[(E - i\Gamma)^2 - \Delta^2]^{1/2}\}|, \quad (2)$$

and the Fermi distribution function, respectively. For the fitting of the superconductor-insulator-normal-metal (SIN) tunneling [Fig. 1(c)], which was also obtained in our break-junction measurements, we can put $N(E+eV, \Gamma)$ in Eq. (1) to be constant. In Fig. 1(a), the intensive gap-edge peaks at the biases of $\pm 2.5\text{--}2.6$ mV are accompanied by structures at $\pm 1.2\text{--}1.3$ mV, which are the characteristics of the SIS tunneling of a BCS superconductor.⁷ The junction resistance of $R_j \approx 0.5$ k Ω at high biases is much lower than the resistance quantum $h/2e^2 \approx 12.9$ k Ω , which is believed to distinguish between the point contact and the vacuum tunneling regimes. The low- R_j value for the tunneling is probably due to a large effective junction area. We compare the experimental data with the calculated curve for the SIS tunneling in Fig. 1(a) using Eqs. (1) and (2), and obtain fairly good agreement between them using $\Delta=1.28$ meV and $\Gamma=0.2$ meV except

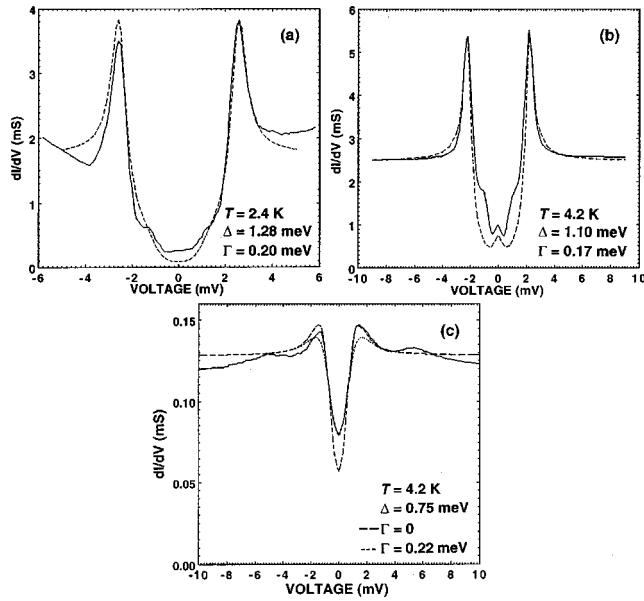


FIG. 1. Tunneling conductance for CeRu_2 from different break junctions. Solid and dashed curves represent, respectively, the experimental data and calculation using Eqs. (1) and (2). Frames (a) and (b) are the SIS tunneling, while (c) is the SIN tunneling.

for the zero-bias region. The fitted value of $4\Delta = 5.12$ meV agrees with the observed peak-to-peak separation of $dI(V)/dV$, $4\Delta_{\text{p-p}} = 5.1$ meV. This is a characteristic feature of SIS tunneling. The subgap structures at $\pm\Delta/e = \pm 1.2$ – 1.3 mV can be due to the two-particle tunneling and/or the SIN tunneling component rather than the density-of-states effect, because they are much enhanced in the experimental data than the calculation. In Fig. 1(b), the experimental curve possesses much leakage inside the gap compared to that for SIS tunneling, but at higher biases the agreement is satisfactory between them. The fitted SIS gap value of $4\Delta = 4.4$ meV again agrees with the observed value of $4\Delta_{\text{p-p}}$. The $dI(V)/dV$ curve in Fig. 1(c) possesses broad gap peaks at ± 1.3 mV, above which broad maxima at ± 5 – 5.2 mV with the conductance background having $R_J \approx 8$ k Ω are seen. The bias positions of the gap peaks are lower than those of Fig. 1(b) in spite of the same temperature of 4.2 K. We have assumed this feature to be due to SIN tunneling; then, the conductance fitting has been performed using the SIN expression based on Eqs. (1) and (2). As shown in Fig. 1(c), the calculated curve with $\Delta = 0.75$ meV and $\Gamma = 0$ agrees with the experimental data around the conductance peaks. We also present the calculated curve with $\Gamma = 0.22$ meV. In this case the magnitude of the observed zero-bias conductance is reproduced, but it does not explain the observed intensive conductance peaks. In SIN tunneling, the proper energy-gap value should be obtained by the value of Δ from the fitting procedure because of the significant thermal broadening of the tunneling density of states. The occurrence of SIN tunneling in the break junction is presumably due to a cracking at the grain boundaries, of which one side is not superconducting.⁴ Since the conductance curve deviates from $N(E, \Gamma)$ only in the low-bias regions, the bias dependence of the background conductance should be taken into account to

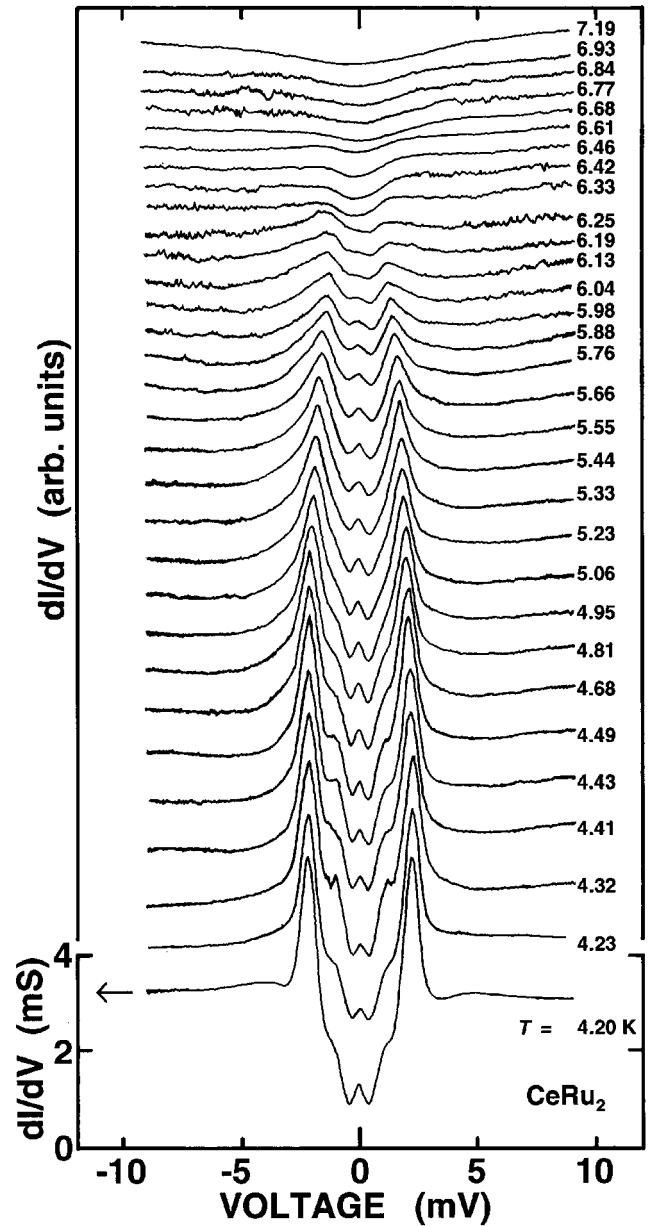


FIG. 2. Temperature variations of the SIS tunneling conductance for CeRu_2 .

make an agreement of the depressed area below the normal-state conductance with the sum areas of the two conductance peaks above it.

In Fig. 2, the temperature variations of the tunneling conductance are shown for the junction of Fig. 1(b). The changes in $dI(V)/dV$ with temperature resemble what we see in the SIS tunnel junction of a BCS superconductor. The subgap leakage is partially explained by Γ and the thermal broadenings, but it is still larger than these effects at every temperature. The subgap structures at $\pm\Delta/e$ merge into the slope in the main gap at ≈ 5.3 K, whereas the zero-bias peak smeared out above 6.1 K. The main gap structures remain up to 6.7 K, that is, well above the bulk $T_c = 6$ K of this sample as described above.

The temperature dependence of the gap magnitudes of Fig. 2 is plotted in Fig. 3. Because of the SIS junction geometry, the gap value at every temperature can be directly

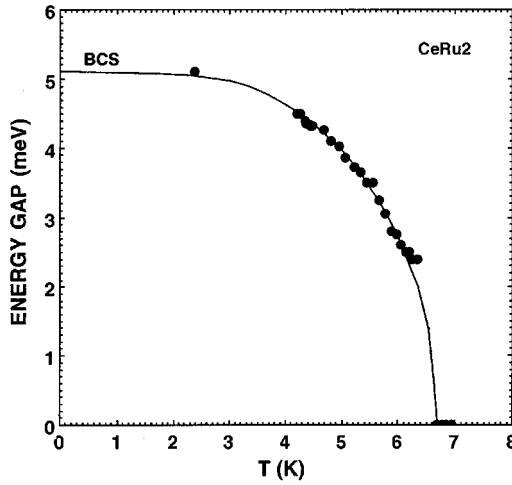


FIG. 3. Temperature dependence of the energy gap $4\Delta_{p-p}$ from Fig. 2. The solid curve represents the BCS prediction.

obtained from the well-defined values of $4\Delta_{p-p}$. The observed temperature dependence of $4\Delta_{p-p}$ is in good agreement with the scaled BCS curve with $4\Delta_{p-p}(0)=5.1$ meV and $T_c=6.7$ K. These values give the ratio $2\Delta(0)/k_B T_c=4.4$, which well exceeds the weak-coupling BCS ratio of 3.5. This is consistent with the value ≈ 4.2 obtained from the specific-heat jump $\Delta C/\gamma T_c \approx 0.115[2\Delta(0)/k_B T_c]^2=2$ (Ref. 2) and ≈ 4 from the NMR measurement.³ Since this ratio is like that for Pb having a similar T_c value, a strong electron-phonon interaction could be expected in CeRu₂. The tunneling data in Figs. 1 and 2, however, do not show such strong-coupling structures, at least below the biases of ± 9 mV. The reasons for the absence of them might be due to the complicated phonon spectra in the Laves-phase C15 crystal structure of CeRu₂. The rather high bulk resistivity of CeRu₂ also could smear out the phonon structures in the tunneling conductance.

In Fig. 4, the temperature variations of $dI(V)/dV$ in Fig. 1(c) are shown. With increasing temperature, gap structures of ± 1.3 mV are broadened and disappear near 5.4 K. There is no shift of the conductance-peak voltages upon warming because of the thermal smearing of the SIN junction geometry. The inset of Fig. 4 shows the temperature dependence of the normalized zero-bias conductance $[dI/dV(0 \text{ mV})]/[dI/dV(10 \text{ mV})]$. This is proportional to the thermally smeared density of states at the Fermi energy, and its smallness at low temperatures measures quality of the junction. The T_c is definitely determined to be 5.42 K from this plot, which is lower than the bulk one. From the fitted value of $2\Delta(4.2 \text{ K})=1.5$ meV in Fig. 1(c), $2\Delta(0)$ is extrapolated to be 1.9–2 meV assuming the BCS temperature dependence of the gap with $T_c=5.42$ K. The ratio $2\Delta(0)/k_B T_c=4.1$ – 4.3 is thus obtained. The asymmetry in the background conductance becomes noticeable above ≈ 5 K due to a slight change in the junction. The outer structures of ± 5 – 5.2 mV remain at least up to 6.5 K, that is, well above the T_c value of this gap, suggesting that these are not related to each other. The value of 5–5.2 meV is still much larger than the expected gap value from the possible local highest T_c of 7.2 K.⁶

It would be interesting to compare the ratio $2\Delta(0)/$

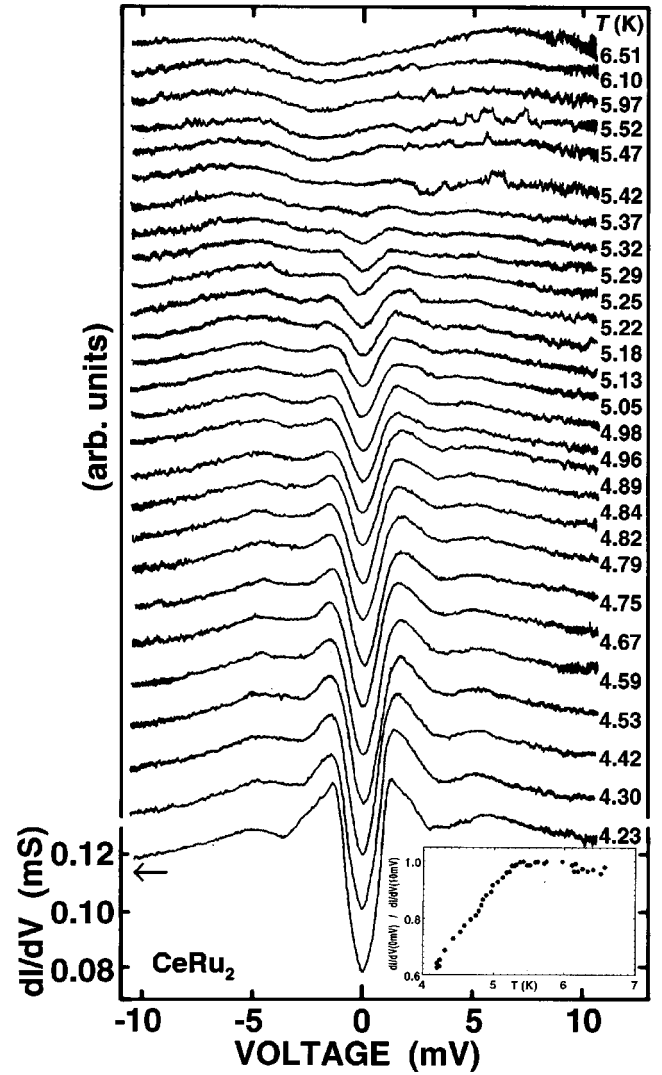


FIG. 4. Temperature variations of the SIN tunneling conductance for CeRu₂. Inset: the temperature dependence of $[dI/dV(0 \text{ mV})]/[dI/dV(10 \text{ mV})]$.

$k_B T_c=4.1$ – 4.4 for CeRu₂ with that of the other intermetallics. This ratio is similar to that of the well-known A15 intermetallic superconductor Nb₃Ge, but its T_c is high ($T_c=21$ K) and thus the strong-coupling phonon structures are clearly observed in the tunneling conductance.⁷ There have been a few successful tunneling measurements on the superconductors containing f electrons to date. The ferromagnetic superconductor ErRh₄B₄ showed the ratio ≈ 3.8 with $T_c=8$ K.⁹ For the heavy-fermion superconductors, UPd₂Al₃ possesses a distinct gap feature having a ratio of ≈ 3.8 with $T_c=2$ K.¹⁰ The compound UBe₁₃ also exhibits a ratio of ≈ 4.2 with $T_c=0.8$ K.¹¹ The strong-coupling ratio of CeRu₂ is quite similar to them, although CeRu₂ is not considered to be a heavy-fermion superconductor. Further, the electron-spectroscopy¹² and band-structure calculations¹³ suggest the substantial weight of a $4f^1$ configuration, and the Ce valence is estimated to be ≈ 3.7 from the bulk measurements.¹⁴ Therefore, it would be plausible that the $4f$ electrons contribute to the strong-coupling ratio of the superconductivity in CeRu₂ to some extent.

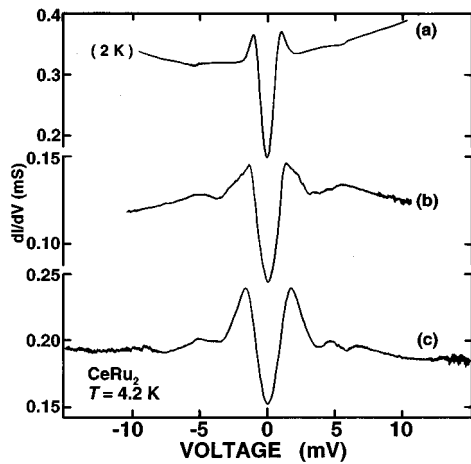


FIG. 5. Tunneling conductance for CeRu_2 from different break junctions.

The reproducible conductance structures observed at ± 5 – 5.2 mV are presented in Fig. 5. These curves were taken from three different break junctions. The curve (b) is the same as Figs. 1(c) and 4. Both the strong-coupling effect of the electron-phonon interaction and the higher harmonics of the gap energy can be ruled out for the origin of these structures because they do not depend on the gap-edge voltages between 1.9 (a) and 3.4 (c) meV. One of the possible origins is associated with the antiferromagnetic phase below $T_N \approx 40$ – 50 K found by susceptibility¹ as well as μSR (muon spin relaxation) (Ref. 15) measurements, which coexists with superconductivity. From this viewpoint, it is interesting to point out that the ratio of $T_c/T_N \approx 0.13$ – 0.17 in CeRu_2 is

close to that for the heavy-fermion superconductors, although the temperature scales are ≈ 10 times larger than those for the heavy-fermion compounds. Nass *et al.*¹⁶ predicted the tunneling structures of the magnetic excitations in the superconducting density of states having a characteristic energy corresponding to the magnetic ordering temperature. In terms of this interpretation, the observed conductance structure at ≈ 5 meV (≈ 58 K) which is close to $k_B T_n$ could be due to the interaction between conduction electrons and magnetic excitations, although there is no signature in the resistivity at T_N . Another interpretation of these structures can be given by the collective excitations (e.g., antiferromagnetic gap) because the ratio $eV_{\text{p-p}}/k_B T_N \approx 3$ approximately agrees with the mean-field value, where $V_{\text{p-p}} \approx 10$ mV is the peak-to-peak separation of the structures. A small amount of the magnetic impurity phase also cannot be ruled out as an origin of these structures.

In summary, we have observed the superconducting energy gap in CeRu_2 using break junctions which are effective to the reactive surface characteristics of the Ce intermetallics. The observed conductance features can be fitted with the BCS density of states for the best data. The temperature dependence of the gap is in good agreement with the BCS prediction. The gap values of $2\Delta(0) = 1.9$ – 2.6 meV with $T_c = 5.4$ – 6.7 K give the ratio $2\Delta(0)/k_B T_c = 4.1$ – 4.4 , indicating a strong-coupling superconductor. This ratio is similar to that of some f -electron superconductors. We could not observe the phonon structures in spite of the strong-coupling ratio. Instead, the reproducible structures are observed at ± 5 – 5.2 mV.

This work was supported by a Grant-in-Aid for Scientific Research from the Ministry of Education, Science, Sports and Culture, Japan.

- ¹T. Nakama, M. Hedo, T. Maekawa, M. Higa, R. Resel, H. Sugawara, R. Settai, Y. Onuki, and K. Yasasaki, *J. Phys. Soc. Jpn.* **64**, 1471 (1995).
- ²A. D. Huxley, C. Paulsen, O. Laborde, J. L. Tholence, D. Sanchez, A. Junod, and R. Calemczuk, *J. Phys.: Condens. Matter* **5**, 7709 (1993).
- ³K. Matsuda, Y. Kohori, and T. Kohara, *J. Phys. Soc. Jpn.* **64**, 2750 (1995).
- ⁴T. Ekino, H. Fujii, M. Kosugi, Y. Zenitani, and J. Akimitsu, *Phys. Rev. B* **53**, 5640 (1996).
- ⁵K. Yagasaki, M. Hedo, and T. Nakama, *J. Phys. Soc. Jpn.* **62**, 3825 (1993).
- ⁶R. N. Shelton, A. C. Lawson, and K. Baberschke, *Solid State Commun.* **24**, 465 (1977).
- ⁷E. L. Wolf, *Principles of Electron Tunneling Spectroscopy* (Oxford University Press, New York, 1985).

- ⁸R. C. Dynes, V. Narayanamurti, and J. P. Garno, *Phys. Rev. Lett.* **41**, 1509 (1978).
- ⁹L.-J. Lin, A. M. Goldman, A. M. Kadin, and C. P. Umbach, *Phys. Rev. Lett.* **51**, 2151 (1983).
- ¹⁰M. Jourdan, M. Huth, J. Hessert, and H. Adrian, *Physica B* **230–232**, 335 (1997).
- ¹¹J. Moreland and A. F. Clark, *Physica B* **194–196**, 1727 (1994).
- ¹²S. H. Yang, H. Kumigashira, T. Yokoya, A. Chainani, T. Takahashi, H. Takeya, and K. Kadowaki, *Phys. Rev. B* **53**, R11 946 (1996).
- ¹³A. Yanase, *J. Phys. F* **28**, 871 (1983).
- ¹⁴J. G. Huber and M. Hakimi, *Bull. Am. Phys. Soc.* **28**, 871 (1983).
- ¹⁵A. D. Huxley, P. D. de Reotier, A. Yaouanc, D. Caplan, M. Couach, P. Lejay, P. C. M. Gubbens, and A. M. Mulders, *Phys. Rev. B* **54**, R9666 (1996).
- ¹⁶M. J. Nass, K. Levin, and G. S. Grest, *Phys. Rev. Lett.* **45**, 2070 (1980).